Geometry of phase separation

Alberto Sicilia,[1] Yoann Sarrazin,[1] Jeferson J. Arenzon,[2] Alan J. Bray,[3] and Leticia F. Cugliandolo[1]
[1]*Université Pierre et Marie Curie–Paris VI, LPTHE UMR 7589, 4 Place Jussieu, 75252 Paris Cedex 05, France*
[2]*Instituto de Física and INCT-Sistemas Complexos, Universidade Federal do Rio Grande do Sul, CP 15051, 91501-970 Porto Alegre, RS, Brazil*
[3]*School of Physics and Astronomy, University of Manchester, Manchester M13 9PL, United Kingdom*
(Received 20 March 2009; published 16 September 2009)

We study the domain geometry during spinodal decomposition of a 50:50 binary mixture in two dimensions. Extending arguments developed to treat nonconserved coarsening, we obtain *approximate* analytic results for the distribution of domain areas and perimeters during the dynamics. The main approximation is to regard the interfaces separating domains as moving independently. While this is true in the nonconserved case, it is not in the conserved one. Our results can therefore be considered as a "first-order" approximation for the distributions. In contrast to the celebrated Lifshitz-Slyozov-Wagner distribution of structures of the minority phase in the limit of very small concentration, the distribution of domain areas in the 50:50 case does not have a cutoff. Large structures (areas or perimeters) retain the morphology of a percolative or critical initial condition, for quenches from high temperatures or the critical point, respectively. The corresponding distributions are described by a $cA^{-\tau}$ tail, where c and τ are exactly known. With increasing time, small structures tend to have a spherical shape with a smooth surface before evaporating by diffusion. In this regime, the number density of domains with area A scales as $A^{1/2}$, as in the Lifshitz-Slyozov-Wagner theory. The threshold between the small and large regimes is determined by the characteristic area $A \sim t^{2/3}$. Finally, we study the relation between perimeters and areas and the distribution of boundary lengths, finding results that are consistent with the ones summarized above. We test our predictions with Monte Carlo simulations of the two-dimensional Ising model.

DOI: 10.1103/PhysRevE.80.031121 PACS number(s): 64.60.Cn, 68.43.Jk

I. INTRODUCTION

Phase separation is the process whereby a binary mixture of components A and B, initially in a homogeneous phase, demix leading to the coexistence of two phases: one rich in A and the other in B. The system, initially in an unstable spatially uniform state, performs a coarsening process to approach its thermodynamically stable phase-separated state [1].

In the case of fluids, hydrodynamic effects may be important to the demixing process [2]; these interactions are hard to treat analytically and the results of numerical simulations are sometimes controversial. Some studies even claim that dynamical scaling is broken by hydrodynamic transport [3]. In the following, we focus on the phase-separation process in systems without hydrodynamics. A typical realization is phase separation in binary alloys, high-viscosity fluids, and polymer blends.

The time-dependent order-parameter characterizing the phase-separation phenomenon is a continuous scalar field $\phi(\vec{r},t)$ that represents the local difference in concentration of the two phases normalized by the sum of the averaged concentrations. Its evolution is described by a phenomenological Langevin-like equation,

$$\frac{\partial \phi}{\partial t} = \vec{\nabla} \cdot \left[M(\phi) \vec{\nabla} \left(\frac{\delta H[\phi]}{\delta \phi} \right) \right] + \eta. \tag{1}$$

$H[\phi]$ is a Ginzburg-Landau-type "free energy" with an elastic term and a double-well potential. The stochastic field $\eta(\vec{r},t)$ represents a thermal noise of zero average and correlator given by

$$\langle \eta(\vec{r},t)\, \eta(\vec{r}',t') \rangle = -2TM\nabla^2 \delta(\vec{r}-\vec{r}')\, \delta(t-t'), \tag{2}$$

while the mobility $M(\phi)$ is in general a function of the field ϕ, as indicated. When $M(\phi)=1$, Eq. (1) is known as the Cahn-Hilliard equation [4] or model B in the Hohenberg-Halperin classification of critical dynamics [5]. Several discrete models to study the phase-separation process in binary alloys have also been proposed and studied in the literature. These are lattice gases that are themselves mapped onto Ising models with locally conserved order parameter [6,7]. The dynamics follow stochastic rules for the interchange of nearest-neighbor A and B molecules or, in the spin language, the reversal of a pair of neighboring antiparallel spins.

Two microscopic processes contribute to phase ordering dynamics with locally conserved order parameter, namely, *bulk* and *surface* diffusion. In bulk diffusion, a molecule separates (evaporation) from the surface of a domain, diffuses within the neighboring domain of the opposite phase, and finally attaches to its original domain or another one. In the context of an Ising-model simulation, there is an activation energy for this process and one can check that the dominant growth mechanism is the transport of material through the bulk from domain boundaries with *large* curvature to domain boundaries with *small* curvature. In surface diffusion, molecules "walk" on the interface. This mechanism leads to the motion of whole domains in the sample and, thus, the possibility of merging two domains together when they collide. In the usual Kawasaki [6] spin-exchange dynamics or in model B's evolution [8], the early dynamics is surface diffusion driven and at a later time the dominant process becomes bulk diffusion. There exist, however, modi-

fied versions where either bulk or surface diffusion is suppressed [8–10].

For deep temperature quenches $M(\phi)\to 0$, bulk diffusion is effectively eliminated and domain growth proceeds by surface motion. In quenches to moderate subcritical temperatures, on the other hand, the mobility does not play an important role $M(\phi)\simeq$const and the domain growth is bulk driven.

Let us now review in some detail the main features of coarsening with locally conserved order parameter. Using the Cahn-Hilliard equation, it can be easily shown that the radius $R(t)$ of a *single spherical* domain of negative phase ($\phi=-1$) in an infinite sea of positive phase ($\phi=+1$) evolves from time $t=0$ to time t as [1]

$$R^3(t) = R^3(0) - \frac{3}{2}\sigma t, \tag{3}$$

with σ a parameter that quantifies the surface tension. A domain with initial radius R_i thus evaporates in a time $t\sim R_i^3$ in contrast to the nonconserved order-parameter dynamics in which the area within a boundary simply shrinks under the curvature force in a time $t\sim R_i^2$ [11].

Lifshitz-Slyozov [12] and Wagner [13] studied, for a *three-dimensional* system, the growth and shrinkage of domains of one phase embedded in one large domain of the other phase in the limit of small minority phase concentration $c\to 0$. In their celebrated papers, they realized that domain growth at the late stages is limited by matter diffusion through the majority domain. In this case, the evolution of a domain of the minority phase with radius R_i immersed in a sea of the majority phase that is "supersaturated" with the dissolved minority species [1,12] can follow two paths: the domain evaporates by diffusion if $R_i<R_c$ or it grows by absorbing material from the majority phase if $R_i>R_c$, where R_c is a time-dependent "critical radius." This critical radius turns out to be the only characteristic length scale in the system $R(t)$ and serves to scale all correlation functions according to the dynamic scaling hypothesis. It grows as $R(t)=R_c(t)\sim t^{1/3}$.

Lifshitz-Slyozov [12] also derived an expression for the density of droplets of the minority phase with linear size R in $d=3$. Three important properties of the Lifshitz-Slyozov distribution are:

(i) The distribution of droplet radii has an upper cutoff $R_{\max}(t)$, where $R_{\max}(t)\sim t^{1/3}$ is a constant, equal to 3/2, times the critical radius $R_c(t)$.

(ii) The decay close to the cutoff is exponential.

(iii) The density of small objects $R\sim 0$ satisfies scaling and behaves as $n(R,t)\sim R_c(t)^{-4}[R/R_c(t)]^2$, where $n(R,t)dR$ is the number of droplets per unit volume with radius in the interval $(R,R+dR)$.

Later simulations established that the scaling functions depend on the minority concentration [14,15].

The Lifshitz-Slyozov calculation can easily be extended to any space dimension $d>2$ [16]. However, the limit $d\to 2$ is singular and does not commute with the limit $c\to 0$. Rogers and Desai [17] showed, however, that the usual scaling forms apply in $d=2$, with $R(t)\sim t^{1/3}$, for large t at small nonzero volume fraction c.

More recently, Huse used scaling and energetic arguments to generalize the Lifshitz-Slyozov growth law and argued that it should also apply to critical quenches with equal volume fractions of the two phases [18]. Numerical simulations [18,19], in agreement also with the earlier ones in [7], suggest that the typical domain radius scales in time as $R(t)\sim t^{1/3}$ for any value of c, even in the 50:50 case. The scaling function for the distribution of domain areas has not been analyzed in this case.

If we take also into account the competition between bulk and surface diffusion, the growth law is modified at early times. The former process is the one responsible for the scaling of global observables with a *typical* domain length $R(t)\sim t^{1/3}$, while the latter yields a slower time dependence $R(t)\sim t^{1/4}$, that is, important only at relatively short times after the quench [20–22]. The temperature-dependent crossover can be seen, for example, in numerical simulations with Kawasaki dynamics [8]. The crossover time diverges when $T\to 0$. This observation has been used to develop accelerated algorithms to simulate discrete models in which only bulk-diffusion processes are considered, which should describe phase separation correctly at late times after the quench.

Phase separation in the Kawasaki spin-exchange dynamics is equivalent to a Cahn-Hilliard equation with order-parameter-dependent mobility. In [10], a model with $M(\phi)=1-\alpha\phi^2$ was studied. The time-dependent structure factor exhibits dynamical scaling, and the scaling function is numerically indistinguishable from the Cahn-Hilliard one, consistent with what was expected from numerical studies with Kawasaki dynamics.

In this paper, we study the morphology of domain and perimeter structures in the spinodal decomposition of a two-dimensional system with *equal concentrations* of the two phases. In particular, we analyze the distributions of the domain areas and their associated perimeters and the relation between areas and perimeters during the evolution. We consider bulk-and-surface diffusion and just-bulk-diffusion processes.

Extending a formalism previously developed for the study of domain growth in the nonconserved case [23–25], we propose an analytic form for the domain size distribution function in its full range of variation, and we test it with simulations on the two-dimensional Ising model (2DIM). Our analytic prediction for the distribution of small areas is the result of one hypothesis: that interfaces move independently. This assumption is valid for domains of any size in curvature-driven dynamics: the fission of a big domain into two smaller ones or the coalescence of two domains to form a bigger one is forbidden in the continuous Allen-Cahn description [11] and is not important in the heat-bath dynamics of the Ising model with nonconserved order parameter. In the conserved order-parameter case, even with $c\to 0$, this assumption does not strictly hold and corrections must, in principle, be included. Indeed, already Lifshitz and Slyozov made an attempt to go beyond their simple model and account for coalescence when $c\to 0$. Later, it became clear that in locally conserved order-parameter dynamics, the dominant effect not accounted for in the simple description that takes

domain boundaries as independent objects was interdomain correlations rather than coalescence. For a discussion of the limit $c \to 0$ considering interactions between droplets, see [26].

Therefore, our analytical results are just a first-order approximation. Still, as we shall see in the main body of the paper, this approximation yields a very good description of numerical data obtained with Monte Carlo (MC) simulations. The quantities on which we focus are domain areas and "hull-enclosed areas," where the latter is the areas enclosed within the outer boundaries (or "hulls") of domains and domain perimeters. The distribution functions for the hull-enclosed and domain areas are $n_{h,d}(A,t)$, where $n_{h,d}(A,t)dA$ is the number of hulls (h) or domains (d) per unit area of the system with area in the range $(A, A+dA)$.

The main properties of these distributions are:

(i) The number density of domain and hull-enclosed areas satisfy scaling $n_{h,d}(A,t)=t^{-4/3}f_{h,d}(A/t^{2/3})$. The argument of the scaling functions arises from the fact that the characteristic area of hulls and domains grows as $t^{2/3}$. The prefactor $t^{-4/3}$ follows from the fact that there is of order one domain per scale area.

(ii) The scaling functions $f_{h,d}(x)$ do not have any cutoff and extend to infinite values of x falling off as $(2)c_{h,d}x^{-\tau}$, with $x=A/(\lambda_{h,d}t)^{2/3}$. The constants $c_{h,d}$ are the ones in the initial (or quasi-initial; see below) area distribution, $n_{h,d}(A_i) \sim (2)c_{h,d}/A_i^{\tau}$ for $A_i \to \infty$. The prefactor c_h is known exactly, $c_h=1/8\pi\sqrt{3}$ [27]. The factor of 2 is present when quenching from high temperature $T_0 > T_c$ and is absent when the initial condition is the critical Ising one $T_0=T_c$. The exponent τ depends on whether we consider hull-enclosed ($\tau=2$) or domain areas and, in the latter case, on the initial condition, i.e., infinite or critical temperature. In both cases, it is very close to 2.

(iii) After a quench from high temperature to a sufficiently low-working temperature $T \ll T_c$, the small-argument behavior of the scaling function is $f(x) \propto \sqrt{x}$, in agreement with the Lifshitz-Slyozov-Wagner prediction for the small concentration limit. At higher working temperature and for critical initial conditions, the behavior is modified in a way that we describe in the text.

The paper is organized as follows. In Sec. II we describe an approximate analytic derivation of the time-dependent hull-enclosed and domain area distributions. These arguments do not rely on any scaling hypothesis but rather support its validity. We compare our approach to the celebrated Lifshitz-Slyozov-Wagner theory [12,13]. In Sec. III we show our numerical results for the statistics of areas in the 2DIM evolving with locally conserved dynamics. We use variants [9] of the Kawasaki algorithm [6] that we briefly explain in this section. The use of different algorithms allows us to switch surface diffusion on and off and pinpoint the relative importance of these processes. Section IV is devoted to the analysis, both analytical and numerical, of the geometry of domain walls during the dynamics and their relation to the corresponding areas. Finally, in the conclusion, we summarize our results and we discuss future studies along these lines.

II. STATISTICS OF AREAS: ANALYTIC RESULTS

In this section, we analyze the number density of hull-enclosed and domain areas. A domain is a region of connected aligned spins. Each domain has one external perimeter, which is called the hull. The hull-enclosed area is the total area within this perimeter, i.e., the domain area plus the area of any internal subdomains.

A. Initial distribution

We study the coarsening dynamics after a quench from $T_0 \to \infty$ and $T_0=T_c$. The first case is very similar to critical percolation, as we explained in [23]. Equilibrium infinite-temperature initial conditions (fraction of up spins$=1/2$) are below the critical random percolation point ($p_c \approx 0.59$) for a square lattice in $d=2$. After a few MC steps, however, the system reaches the critical percolation condition, e.g., the expected A^{-2} tail is observed in the distribution of hull-enclosed areas. We have checked that this is so from the analysis of several correlation functions as well as the distribution of structures. The same happens for nonconserved order-parameter dynamics [23], where a detailed discussion can be found. This fact justifies the use of the Cardy-Ziff exact result for the distribution of hull-enclosed areas at critical percolation [27] as our effective initial condition from $T_0 \to \infty$. From a more general perspective, one can argue that if the system is coarse grained to the scale $R(t)$ and $R(t)$ is large compared to the lattice spacing, a continuum description becomes appropriate, for which the percolation threshold is precisely 1/2. At the scale $R(t)$, the system is disordered and has the character of the percolation model at threshold.

In Sec. II in [23], we recalled the equilibrium distribution of hull-enclosed and domain areas, domain walls, and their geometrical relation to their associated areas at critical percolation and critical Ising initial conditions. In Sec. III we derived some generic results that follow from the use of sum rules and the scaling hypothesis. We do not repeat the description of these properties here but we refer the reader to [23] for further details.

For future reference, we simply list here the initial distributions $n_{h,d}(A_i,t_i)$ of hull-enclosed and domain areas [27–29]. For critical Ising initial conditions, they are

$$n_h(A_i,t_i) = \frac{c_h}{A_i^2},$$

$$n_d(A_i,t_i) = \frac{c_d A_0^{\tau-2}}{A_i^{\tau}}, \quad \tau = \frac{379}{187}, \tag{4}$$

while those describing the critical percolation state are

$$n_h(A_i,t_i) = \frac{2c_h}{A_i^2},$$

$$n_d(A_i,t_i) = \frac{2c_d A_0^{\tau'-2}}{A_i^{\tau'}}, \quad \tau' = \frac{187}{91}. \tag{5}$$

The expression for $n_h(A_i,t_i)$ is asymptotically exact for areas A_i large compared to the microscopic area $A_0 \approx a^2$, where a

is the lattice spacing. The factor of 2 is present for the critical percolation but absent for the critical Ising initial condition [27]. In the former case, the "initial" time t_i is taken to be a few MC steps, such that the system has effectively reached the percolative critical state. The constant c_h is known analytically, $c_h=1/8\pi\sqrt{3}$ [27].

As discussed at length in [23], the domain area distributions must fall off faster than A^{-2} in order that the total domain area, per unit area of the system, be finite (and equal to unity). Indeed the exponents τ and τ' in Eqs. (4) and (5) take the numerical values $\tau \simeq 2.027$ and $\tau' \simeq 2.055$.

B. Characteristic domain length

It is by now well established [12,18] that the spatial equal-time correlation function in demixing systems is correctly described by the dynamic scaling hypothesis with a characteristic length $R(t) \sim t^{1/3}$ in agreement with the Lifshitz-Slyozov-Wagner prediction [12,13] and the extension beyond the small concentration limit derived by Huse [18]. The effect of temperature fluctuations is expected to be described by a T-dependent prefactor $R(t,T)=[\lambda(T)t]^{1/3}$. In the following, we do not write the T dependence explicitly.

C. Large structures

It is natural to assume that at time t, as for nonconserved order-parameter dynamics, large structures characterized by a long linear dimension $R_i \gg R(t)$ have not changed much with respect to the initial condition. We shall support this claim with the numerical results. Thus, for sufficiently large hull-enclosed areas such that the time dependence can be neglected, we expect

$$n_h(A,t) \approx \frac{c_h}{A^2}, \quad A \gg (\lambda_h t)^{2/3}, \tag{6}$$

for Ising critical conditions and with a prefactor 2 for high-temperature ones.

Similarly, for large domains, the area dependence of their distribution follows that of the initial condition [Eqs. (4) and (5)].

D. Small structures

Small structures, such that $R_i \ll R(t)$, are mostly embedded in very large domains. To a first approximation, we shall assume that they are *independent*. Moreover, they are not expected to have holes of the opposite phase within, implying the equivalence between hull-enclosed and domain areas at these scales. Indeed, any smaller structure placed within must have evaporated by time t. We then propose that the number density of *small* hull-enclosed or domain areas at time t can be written as a function of the initial distribution,

$$n(A,t) \approx \int_0^\infty dA_i \delta[A - A(t,A_i)] n(A_i,t_i), \tag{7}$$

with A_i the initial area and $n(A_i,t_i)$ their number density at the initial time t_i. $A(t,A_i)$ is the area of a domain at time t that had area A_i at time t_i. In writing this equation, we have implicitly assumed that an area cannot split into two and that two such areas cannot coalesce, which is not strictly true in conserved order-parameter dynamics.

Note that for sufficiently large areas so that the time dependence is not important and $A \sim A_i$, Eq. (7) immediately yields $n(A,t)=n(A_i,t_i)$ and Eq. (6) is recovered. It has to be stressed, however, that Eq. (7) does not strictly apply in this case.

Assuming that the small areas are *circular*

$$A^{3/2}(t,A_i) = A_i^{3/2} - \lambda_h(T)(t - t_i), \tag{8}$$

see Eq. (3), and after a straightforward calculation, using Eqs. (4) and (5) for the initial distribution, one finds

$$(\lambda_h t)^{4/3} n_h(A,t) = \frac{(2)c_h \left[\dfrac{A}{(\lambda_h t)^{2/3}} \right]^{1/2}}{\left\{ 1 + \left[\dfrac{A}{(\lambda_h t)^{2/3}} \right]^{3/2} \right\}^{5/3}} \tag{9}$$

for hull-enclosed areas and Ising critical initial conditions (for high-temperature ones, as usual, we should include the prefactor 2). This prediction has the expected scaling form $n_h(A,t)=t^{-4/3} f(A/t^{2/3})$ corresponding to a system with characteristic area $A(t) \sim t^{2/3}$ or characteristic length scale $R(t) \sim t^{1/3}$. At very small areas, $A \ll (\lambda_h t)^{2/3}$, where our approximations are better justified, one has

$$(\lambda_h t)^{4/3} n_h(A,t) \approx (2) c_h \left[\frac{A}{(\lambda_h t)^{2/3}} \right]^{1/2}. \tag{10}$$

As expected, taking the limit $A/(\lambda_h t)^{2/3} \gg 1$ in Eq. (9), one recovers Eq. (6). Although this limit goes beyond the limit of validity of Eq. (9), we shall propose that Eq. (10) actually holds, at least approximately, for all values of $A/(\lambda_h t)^{2/3}$.

In [23], we studied nonconserved order-parameter dynamics and we derived the number density of domain areas from the one of hull-enclosed areas. The key fact in this case was that we could treat the distribution of hull-enclosed areas *exactly* and then use a small $c_h \simeq 0.023$ expansion to get the statistical properties of domains. In the case of phase separation, our results for hull-enclosed areas are already approximate. Still, the relation between hull-enclosed area distribution and domain area distribution obtained in [23] should remain approximately true, as a first-order expansion in small c_h, since small domains are not expected to have structures within. In conclusion, for large areas and long times such that a regularizing microscopic area $A_0=\lambda_d t_0$ can be neglected, we expect the same functional form as the one given in Eq. (9) with $c_d=c_h+\mathcal{O}(c_h^2)$, $\lambda_d=\lambda_h[1+\mathcal{O}(c_h)]$, and the power 5/3 in the denominator replaced by $(2\tau+1)/3$ or $(2\tau'+1)/3$

$$(\lambda_d t)^{4/3} n_d(A,t) \simeq \frac{(2)c_d \left[\dfrac{A}{(\lambda_d t)^{2/3}} \right]^{1/2}}{\left\{ 1 + \left[\dfrac{A}{(\lambda_d t)^{2/3}} \right]^{3/2} \right\}^{(2\tau+1)/3}} \equiv g(x), \tag{11}$$

with $x=A/(\lambda_d t)^{2/3}$, and

$$(\lambda_d t)^{4/3} n_d(A,t) \simeq (2) c_d \left[\frac{A}{(\lambda_d t)^{2/3}} \right]^{1/2}, \tag{12}$$

for $A \ll (\lambda_d t)^{2/3}$. This expression can be compared to Eq. (49) in [23] valid for nonconserved order-parameter dynamics.

Let us emphasize again the main approximation of our analytical approach: we are considering each domain area as an independent entity. This is strictly true for the nonconserved order parameter [23,24] but is an approximation in the conserved order-parameter problem.

E. Superuniversality

All the results above are valid for the bulk diffusion-driven case. What happens if we consider the case in which bulk and surface diffusion are in competition or whether we include quenched disorder in the couplings? If we suppose that all these systems belong to the same dynamical universality class, the scaling functions being the same, then Eq. (9) can be generalized in the form

$$R^4(t) n_h(A,t) = \frac{(2) c_h \left[\frac{A}{R^2(t)} \right]^{1/2}}{\left\{ 1 + \left[\frac{A}{R^2(t)} \right]^{3/2} \right\}^{5/3}} \tag{13}$$

and similarly for the domain area distribution. The time dependence in $R(t)$ should include all regimes (e.g., $t^{1/4}$ and $t^{1/3}$ in the clean case with surface and bulk diffusion) and can be extracted from the dynamic scaling analysis of the correlation functions. We shall check numerically the superuniversality hypothesis.

III. STATISTICS OF AREAS: NUMERICAL TESTS

To test our analytic results, we carried out numerical simulations on the 2D square-lattice Ising model (2DIM) with periodic boundary conditions,

$$H = -\sum_{\langle i,j \rangle} J_{ij} \sigma_i \sigma_j, \tag{14}$$

where $\sigma_i = \pm 1$. We will start considering the pure model $J_{ij} = J > 0 \, \forall \, ij$ and then the random-bond model in which the J_{ij}'s are random variables uniformly distributed over the interval [1/2, 3/2]. We used several versions of conserved order-parameter dynamics that switch on and off surface diffusion. These are Kawasaki dynamics at finite temperature, including both surface and bulk diffusion, and accelerated bulk diffusion in which surface diffusion is totally suppressed. Bulk diffusion needs to overcome energy barriers; thus, this variant runs at finite temperature only. In all cases, we implemented the continuous time method and the algorithms become rejection free. A detailed description of these algorithms appeared in [9]. Domain areas are identified with the Hoshen-Kopelman algorithm [30].

All data have been obtained using systems with size $L^2 = 10^3 \times 10^3$ and 10^3 runs using independent initial conditions. We ran at different temperatures specified below. We considered two types of initial conditions, equilibrium at infinite temperature $T_0 \to \infty$ and equilibrium at the critical Ising temperature $T_0 = T_c$. All results are presented in equivalent MC times. An example, for $T_0 \to \infty$, is presented in Fig. 1, with snapshots taken at different times.

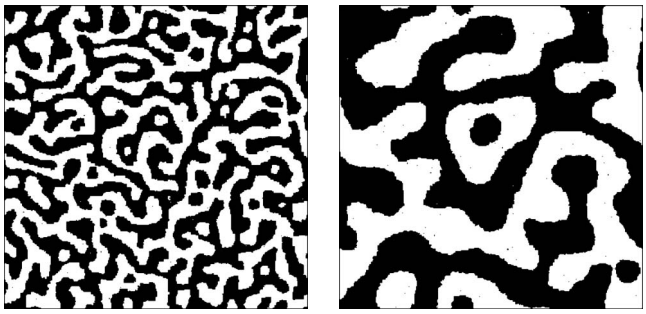

FIG. 1. Snapshots of the 2D Ising model evolving with a locally conserved order parameter at $t=1000$ and $t=16\,000$ equivalent MC steps using the accelerated bulk algorithm explained in Sec. III. The initial condition is a random configuration of ± 1 spins taken with probability one half, that is to say, an infinite-temperature state. Evolution occurs at $T=1.0$.

Domain areas

In this section, we show data obtained with the accelerated bulk-diffusion algorithm, but we checked that similar results are obtained with finite-temperature Kawasaki dynamics.

1. Infinite-temperature initial condition, low T evolution

In Fig. 2 (top), we show the time-dependent domain area distribution in double-logarithmic scale, at three different times, following a quench from $T_0 \to \infty$ to $T=1.0$. The working temperature is very low compared to the critical value $T_c = 2.269$.

The figure shows a strong time dependence at small areas and a very weak one in the tail, which is clearly very close to a power law. The curves at small areas move downward and the breaking point from the asymptotic power-law decay moves toward larger values of A for increasing t. We include the spanning domain in the statistics: the bump on the tail of the distribution is a finite-size effect visible only when the number of domain areas has already decreased by several orders of magnitude. In the tail of the probability distribution function, the numerical error is smaller than the size of the data points. The discussion of finite-size effects in [23] also applies to this case.

We test the analytic prediction: the very good agreement between the analytical theory and the data is quite impressive. In Fig. 2 (bottom), we scale the data by plotting $(\lambda_d t)^{4/3} n_d(A,t)$ against $A/(\lambda_d t)^{2/3}$ with $\lambda_d = 0.008\,3$. For A larger than the "typical" value $(\lambda_d t)^{2/3}$, the time and λ_d dependence become less and less important. We fit the parameter $\lambda_d(T)$ by analyzing the behavior at small areas $A^{3/2} < \lambda_d(T) t$ and we find that $\lambda_d(T=1.0) = 0.008\,3$ yields the best collapse of data. We use the value $c_d = 0.025$ [23]. The full line is our prediction (11).

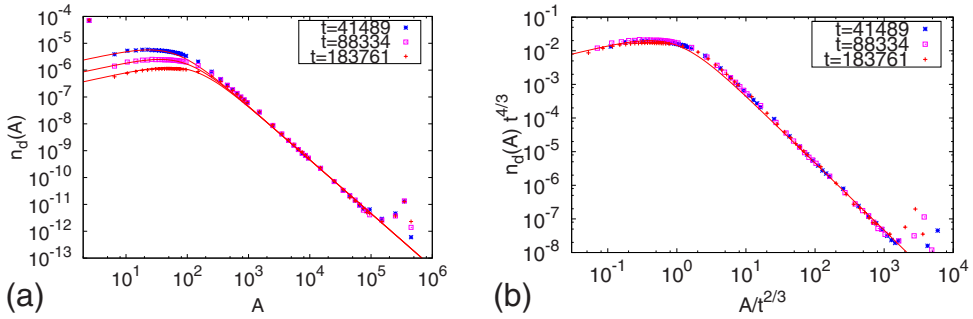

FIG. 2. (Color online) Left panel: number density of domains areas per unit area for the 2DIM evolving at $T=1.0$ after a quench from $T_0 \to \infty$ using the accelerated algorithm. The dotted line represents the analytical prediction. Right panel: rescaled data using the typical domain area time dependence $A \sim t^{2/3}$. The dotted line is the theoretical prediction in Eq. (11) with τ replaced by τ', appropriate to a disordered initial state.

In Fig. 3 we present the domain area distribution for the evolution using the Kawasaki algorithm both for the clean and the disordered systems. The agreement with the analytical prediction is as good as with the bulk-diffusion algorithm, suggesting the validity of superuniversality between both dynamics.

We extract the growing length $R(t)$ from the analysis of the spatial correlation function [23] and we find very good agreement between the numerical data and the scaling function suggesting that superuniversality with respect to the inclusion of disorder in the interactions also holds.

2. Critical temperature initial condition, low T evolution

We now use a critical Ising initial condition $T_0=T_c$ and show the results in Fig. 4. In this case, we have to further distinguish large and small domain sizes. We find that the distribution at large areas $A \gg (\lambda_d t)^{2/3}$ is well described by the initial condition form. At the crossover $A \sim (\lambda_d t)^{2/3}$, the data points leave the asymptotic power law with parameter c_d to approach the one with $2c_d$. For small areas, $A < (\lambda_d t)^{2/3}$ we find that Eq. (11) is not satisfied (see Fig. 4). Although few data point fall in this regime, the departure from $\sqrt{x}$ is clear.

We believe that the reason why the analytic prediction for small areas fails in this case is that the assumption of independence of small domains is not justified for a critical Ising initial condition.

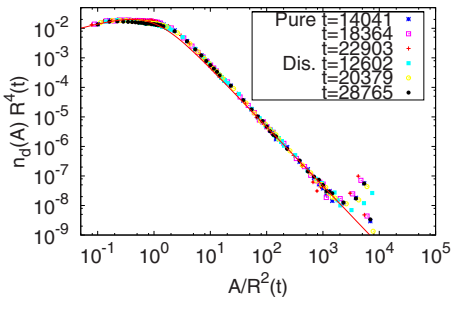

FIG. 3. (Color online) Simulations with the Kawasaki algorithm, without and with disorder. The solid lines represent the analytic prediction with $c_d=0.025$, $\tau'=2.055$, and $\lambda_d=0.3$. For the disordered case, the growth law $R(t)$ is extracted from the spatial correlation function. Even if there are deviations from the theoretical curve, the data seem to show superuniversality.

3. Dependence on the working temperature

Up to now, we showed results obtained using a rather low-working temperature. We now study whether and how our results are modified when using higher values of T. Figure 5 shows the numerical data and proves that the scaling is well satisfied at all times and for all areas. The large scale behavior of the distribution is not modified by T and all data are well described by the initial condition form. Instead, the small scale behavior depends strongly on temperature fluctuations. The anomalous up-rising part of the distribution at small areas is time independent, suggesting that it can be associated with equilibrium fluctuations of the domain walls. As shown in Fig. 5, it is possible to extract the interface thermal fluctuations as was done in Ref. [23] with the bulk equilibrium droplets (see Figs. 20 and 21 of that paper).

IV. STATISTICS OF PERIMETERS AND FRACTAL PROPERTIES

The analytic argument described in Sec. II can be extended to study the distribution of domain-wall lengths or perimeters. The domain perimeter is the total length of the interface between the chosen domain and the neighboring ones—including the hull and internal borders. In this section, we present the analytic prediction for this function together with numerical results that confirm it. We concentrate on $T_0 \to \infty$ and low-working temperature. In the simulations, we

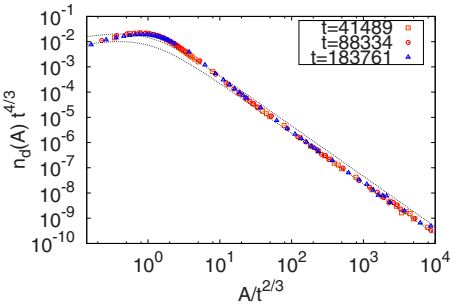

FIG. 4. (Color online) Number density of domain areas per unit area for the 2DIM evolving at $T=1.0$ after a quench from $T_0=T_c$ using the accelerated bulk algorithm. The lines represent Eq. (11) with constant c_d and $2c_d$.

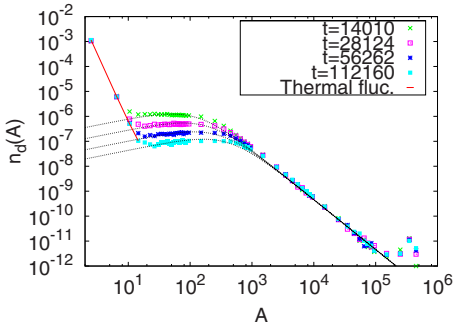

FIG. 5. (Color online) Number density of domains areas per unit area for the 2DIM evolving at $T=1.5$ after a quench from $T_0 \to \infty$ using the accelerated bulk algorithm. The prefactor $\lambda_d(T)$ in the growing length is chosen to be $\lambda_d(T)=0.0060$. Compare to the results shown in Fig. 2 obtained for a lower-working temperature.

define the length of the boundary as the number of broken bonds.

A detailed description of the relation between the domain areas and their boundaries in the critical Ising and critical percolation conditions as well as the number densities of domain perimeters was given in [23]. Here we focus on their evolution.

After a quench from $T_0 \to \infty$, the domain areas A and their corresponding perimeters p obey the scaling relations (see Fig. 6)

$$\frac{A}{(\lambda_d t)^{2/3}} \sim \eta_d' \left(\frac{p}{(\lambda_d t)^{1/3}} \right)^{\alpha_d'}, \tag{15}$$

with

$$\left. \begin{array}{l} \alpha_d'^{>} \sim 1.00 \pm 0.1 \\ \eta_d'^{>} \sim 0.75 \end{array} \right\} \quad \text{for} \quad \frac{A}{(\lambda_d t)^{2/3}} \gtrsim 10, \tag{16}$$

and

$$\left. \begin{array}{l} \alpha_d'^{<} \sim 2.00 \pm 0.1 \\ \eta_d'^{<} \sim 0.045 \end{array} \right\} \quad \text{for} \quad \frac{A}{(\lambda_d t)^{2/3}} \lesssim 10. \tag{17}$$

The relation between areas and perimeters exhibits two distinct regimes with a quite sharp crossover between them. During the coarsening process, a characteristic scale $R(t) \sim (\lambda_d t)^{1/3}$ develops such that domains with area $A > R^2(t)$ have the same exponent as in the initial condition (structures that are highly ramified with $\alpha'^{<} \simeq 1$) and domains with $A < R^2(t)$ become regular ($\alpha'^{<} \simeq 2$). Interestingly, the small structures in the nonconserved order-parameter dynamics are not completely circular, as demonstrated by the fact that their $\alpha'^{<} \simeq 1.8$ (see Fig. 6).

In analogy with the derivation in Sec. II for the time-dependent number density of domain areas, the time-dependent number density of domain-wall lengths $n_d(p,t)$ is given by

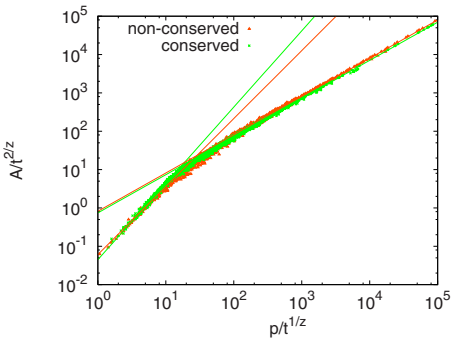

FIG. 6. (Color online) The time-dependent relation between the area and the domain boundary evolving at $T=1.0$ after a quench from $T_0 \to \infty$ using conserved and nonconserved order-parameter dynamics. The lines are fits to the data points. For the large structures, the fit yields $\alpha'^{>} \simeq 1$ in both cases, while for the small structures it yields $\alpha'^{>} \simeq 2$ for conserved order-parameter dynamics (circular domains) and $\alpha'^{>} \simeq 1.8$ for nonconserved order-parameter dynamics. Here $z=2$ and 3 for nonconserved and conserved dynamics, respectively.

$$(\lambda_d t) n_d(p,t) \sim \frac{\alpha_d'^{<} (\eta_d'^{<})^{3/2} 2 c_d \left(\frac{p}{(\lambda_d t)^{1/3}} \right)^{[(3\alpha_d'^{<})-2]/2}}{\left[1 + (\eta_d'^{<})^{3/2} \left(\frac{p}{(\lambda_d t)^{1/3}} \right)^{(3\alpha_d'^{<})/2} \right]^{(2\tau'+1)/3}} \tag{18}$$

for small areas, $A/(\lambda_d t)^{2/3} < 10$, and the same expression with $\eta_d'^{<}$ and $\alpha_d'^{<}$ replaced by $\eta_d'^{>}$ and $\alpha_d'^{>}$ for large areas $A/(\lambda_d t)^{2/3} > 10$. Note that these expressions satisfy scaling. The scaling function $f_<(x)$, with $x = p/(\lambda_d t)^{1/3}$, reaches a maximum at

$$x_{max} = \left(\frac{3\alpha_d'^{<} - 2}{2(\eta_d'^{<})^{3/2} [\alpha_d'^{<} (\tau' - 1) + 1]} \right)^{2/(3\alpha_d'^{<})} \tag{19}$$

and then falls off to zero as another power law. There is then a maximum at a finite and positive value of p as long as $\alpha_d'^{<} > 1$, that is to say, in the regime of not too large areas. The numeric evaluation of the right-hand side yields $x_{max} = p_{max}/(\lambda_d t)^{1/3} \sim 3$, which is in the range of validity of the scaling function $f_<$. The time-dependent perimeter number density for long perimeters falls off as a power law $f_>(x) \sim x^{\alpha_d'^{>}(1-\tau')-1}$. Although the function $f_>$ also has a maximum, this one falls out of its range of validity. The power law describing the tail of the number density of long perimeters is the same as the one characterizing the initial distribution.

In Fig. 7 (top and bottom), we display the time-dependent perimeter number densities for a system evolving at $T=1.0$ after a quench from $T_0 \to \infty$. Notice that the perimeter length definition that we use on the lattice can only take even values and, thus, when constructing the histogram we have to take into account the extra factor of 2 in the binning. The data are in remarkably good agreement with the analytic prediction; the lines represent the theoretical functional forms for long

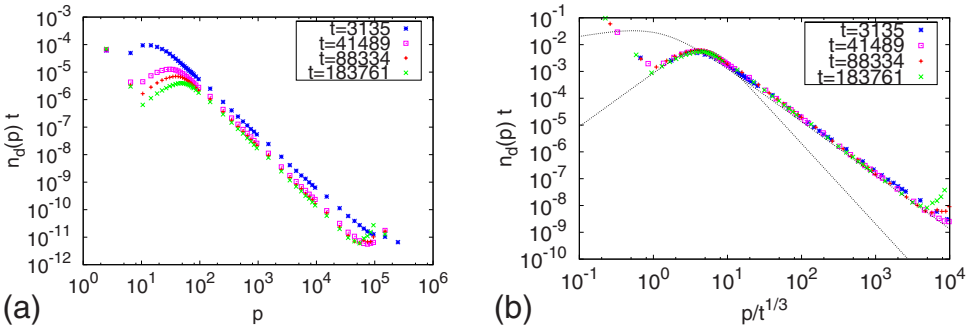

FIG. 7. (Color online) The time-dependent number density of perimeters evolving at $T=1.0$ from an initial condition at $T_0 \to \infty$. Left panel: raw data; note that the time dependence is visible in the whole range of values of p (while in the area number densities, the large area tails were very weakly dependent on time). Right panel: scaled data and analytic predictions for the small and large area regimes.

and short lengths and describe very well the two limiting wings of the number density. The maximum is located at a value that is in agreement with Eq. (19).

V. CONCLUSIONS

In this paper, we studied the statistics and geometry of hull-enclosed and domain areas and interfaces during spinodal decomposition in two dimensions.

The analytical part of our work is an extension of what we presented in [23] for the nonconserved order-parameter case. The numerical part of it deals with Monte Carlo simulations of the 2DIM with locally conserved magnetization. Our main results are:

(i) We derived the scaling functions of the number density of domain areas and perimeters with an approximate analytic argument. The expression that we obtained has two distinct limiting regimes. For areas that are much smaller than the characteristic area $R^2(t)$, the Lifshitz-Slyozov-Wagner behavior is recovered after a quench from $T_0 \to \infty$ and evolving at sufficiently low T. These structures are compact with smooth boundaries, close to circular, since the area-perimeter relation is $A \sim p^2$.

(ii) At higher T, the small area behavior departs from the Lifshitz-Slyozov-Wagner prediction. As for nonconserved order-parameter dynamics, once we subtracted the contribution from thermal domains within the growing structures, the universal prediction is recovered.

(iii) For critical Ising initial conditions, large structures keep the geometry they had initially, but small structures fail to follow our prediction. We conjecture that the reason is that our starting assumption, independence of domain-wall motion for small domains, is not valid due to strong correlations in this case.

(iv) The geometrical properties and distribution of the time-dependent areas that are larger than $R^2(t)$ are the ones of critical continuous percolation (for all initial conditions equilibrated at $T_0 > T_c$) and critical Ising (for $T_0 = T_c$). The long interfaces retain the fractal geometry imposed by the equilibrium initial condition.

These results complement the ones that we presented in [23–25]. It would be interesting to experimentally check these results, as was done for nonconserved dynamics in [31]. It is important to summarize the picture that emerges from all these studies.

Large structures, with an area larger than the typical one $A > R^2$, keep the geometry they had initially in all respects. The scaling functions are thus independent of the dynamics—conserved or nonconserved—and the presence or not of weak disorder.

Small structures do not keep the initial geometry but become more circular in all cases. For a clean system with conserved order parameter, domains are indeed circular, while for nonconserved order parameter they become close to circular. The scaling function of their distribution depends on the type of dynamics considered, but it does not depend on the presence of weak disorder once scaling by the pertinent growth law has been taken into account. In Fig. 8 we illustrate this statement by comparing the number densities of domain areas, on one hand, in the random-bond Ising model (RBIM) with nonconserved order parameter (red data points) and the analytic result for nonconserved order-parameter dynamics and, on the other hand, in the clean and disordered conserved order-parameter dynamics.

Once the superscaling of the number density with respect to weak-quenched randomness is established numerically, we can infer what it implies for the time evolution of the individual small structures under the assumption of independence discussed in the text. Indeed, starting from Eq. (7) one

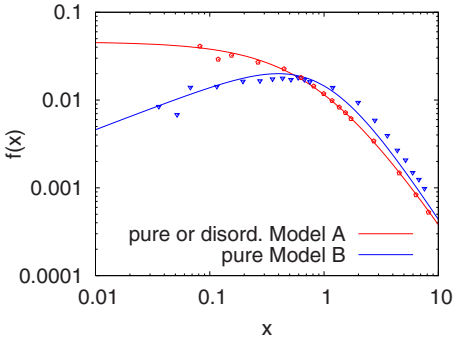

FIG. 8. (Color online) Comparison between the number density of domain areas in the clean and disordered 2D Ising model with nonconserved dynamics and conserved dynamics in a zoom over the small area regime. The data points are the result of the numerical simulations, while the straight lines are the analytic predictions.

can derive Eq. (13) if one assumes that each time-dependent area is linked to the initial value by

$$A^{z/2}(t) \approx A_i^{z/2} - R(t), \tag{20}$$

where $z=2$ for systems in the universality class of model A (e.g., the nonconserved order-parameter dynamics of the RBIM), and $z=3$ for systems in the universality class of model B (e.g., the Kawasaki dynamics). Note that inside each universality class, the growth laws $R(t)$ can be very different.

ACKNOWLEDGMENTS

A.S. and L.F.C. acknowledge financial support from Secyt-ECOS P. Grant No. A01E01 and PICS Grant No. 3172. A.S., J.J.A., and L.F.C. acknowledge financial support from CAPES-Cofecub research Grant No. 448/04. J.J.A. is also partially supported by the Brazilian agencies CNPq and FAPERGS.

[1] see A. J. Bray, Adv. Phys. **43**, 357 (1994), and references therein, for a review of coarsening phenomena.
[2] E. D. Siggia, Phys. Rev. A **20**, 595 (1979).
[3] A. J. Wagner and J. M. Yeomans, Phys. Rev. Lett. **80**, 1429 (1998).
[4] J. W. Cahn and J. E. Hilliard, J. Chem. Phys. **28**, 258 (1958).
[5] P. Hohenberg and B. I. Halperin, Rev. Mod. Phys. **49**, 435 (1977).
[6] K. Kawasaki, Phys. Rev. **145**, 224 (1966); **148**, 375 (1966); **150**, 285 (1966).
[7] A. B. Bortz, M. H. Kalos, J. L. Lebowitz, and M. A. Zendejas, Phys. Rev. B **10**, 535 (1974); J. Marro, A. B. Bortz, M. H. Kalos, and L. L. Lebowitz, *ibid.* **12**, 2000 (1975); M. Rao, M. H. Kalos, J. L. Lebowitz, and J. Marro, *ibid.* **13**, 4328 (1976); A. Sur, J. L. Lebowitz, J. Marro, and M. H. Kalos, *ibid.* **15**, 3014 (1977).
[8] S. van Gemmert, G. T. Barkema, and S. Puri, Phys. Rev. E **72**, 046131 (2005).
[9] M. E. J. Newman and G. T. Barkema, *Monte Carlo Methods* (Oxford University Press, New York, 1999).
[10] S. Puri, A. J. Bray, and J. L. Lebowitz, Phys. Rev. E **56**, 758 (1997).
[11] S. M. Allen and J. W. Cahn, Acta Metall. **27**, 1085 (1979).
[12] I. M. Lifshitz and V. V. Slyozov, J. Phys. Chem. Solids **19**, 35 (1961).
[13] C. Wagner, Z. Elektrochem. **65**, 581 (1961).
[14] S. Puri, Phys. Lett. A **134**, 205 (1988).
[15] R. Toral, A. Chakrabarti, and J. D. Gunton, Physica A **213**, 41 (1995).
[16] J. H. Yao, K. R. Elder, H. Guo, and M. Grant, Phys. Rev. B **47**, 14110 (1993).
[17] T. M. Rogers and R. C. Desai, Phys. Rev. B **39**, 11956 (1989).
[18] D. A. Huse, Phys. Rev. B **34**, 7845 (1986).
[19] J. G. Amar, F. E. Sullivan, and R. D. Mountain, Phys. Rev. B **37**, 196 (1988); T. M. Rogers, K. R. Elder, and R. C. Desai, *ibid.* **37**, 9638 (1988).
[20] G. F. Mazenko, Phys. Rev. B **43**, 5747 (1991).
[21] F. Corberi, A. Coniglio, and M. Zannetti, Phys. Rev. E **51**, 5469 (1995).
[22] G. Szabó, Phys. Rev. E **57**, 6172 (1998).
[23] A. Sicilia, J. J. Arenzon, A. J. Bray, and L. F. Cugliandolo, Phys. Rev. E **76**, 061116 (2007).
[24] J. J. Arenzon, A. J. Bray, L. F. Cugliandolo, and A. Sicilia, Phys. Rev. Lett. **98**, 145701 (2007).
[25] A. Sicilia, J. J. Arenzon, A. J. Bray, and L. F. Cugliandolo, EPL **82**, 10001 (2008).
[26] M. Marder, Phys. Rev. A **36**, 858 (1987).
[27] J. Cardy and R. M. Ziff, J. Stat. Phys. **110**, 1 (2003).
[28] D. Stauffer and A. Aharony, *Introduction to Percolation Theory*, 2nd ed. (Taylor & Francis, London, 1994).
[29] A. L. Stella and C. Vanderzande, Phys. Rev. Lett. **62**, 1067 (1989).
[30] J. Hoshen and R. Kopelman, Phys. Rev. B **14**, 3438 (1976).
[31] A. Sicilia, J. J. Arenzon, I. Dierking, A. J. Bray, L. F. Cugliandolo, J. Martinez-Perdiguero, I. Alonso, and I. C. Pintre, Phys. Rev. Lett. **101**, 197801 (2008).